AVS JVSTB Journal of Vacuum Science & Technology B

Correlation between the chemical compositions and optical properties of $AlSi_xN_y$ embedded layer for attenuated phase-shifting mask in 193 nm and the modification of the R–T method for measuring n and k

Cheng-ming Lin and Wen-an Loong

Citation: Journal of Vacuum Science & Technology B **18**, 3371 (2000); doi: 10.1116/1.1319835
View online: http://dx.doi.org/10.1116/1.1319835
View Table of Contents: http://scitation.aip.org/content/avs/journal/jvstb/18/6?ver=pdfcov
Published by the AVS: Science & Technology of Materials, Interfaces, and Processing

Articles you may be interested in

Ultrathin TiO_2 amorphous films for high transmittance APSM blanks at 157 and 193 nm wavelength simultaneously
J. Vac. Sci. Technol. B **21**, 3062 (2003); 10.1116/1.1624252

Fabry–Pérot structures for attenuated phase-shifting mask application in ArF and F_2 lithography
J. Vac. Sci. Technol. B **21**, 3057 (2003); 10.1116/1.1624251

Optical-constant tunable $(ZrO_2)_x/(Cr_2O_3)_y/(Al_2O_3)_{1-x-y}$ optical superlattices for attenuated phase shift mask in ArF lithography
J. Vac. Sci. Technol. B **19**, 2617 (2001); 10.1116/1.1408951

F-doped and H_2-impregnated synthetic SiO_2 glasses for 157 nm optics
J. Vac. Sci. Technol. B **17**, 3280 (1999); 10.1116/1.590995

Characteristics of plasma enhanced chemical vapor deposition-grown SiN_x films prepared for deep ultraviolet attenuated phase-shifting masks
J. Vac. Sci. Technol. B **16**, 3612 (1998); 10.1116/1.590314

Re-register for Table of Content Alerts

Create a profile.

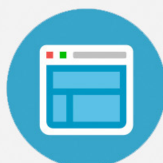

Sign up today!

Redistribution subject to AVS license or copyright; see http://scitation.aip.org/termsconditions. Download to IP: 140.113.38.11 On: Thu, 01 May 2014 07:40:58

Correlation between the chemical compositions and optical properties of $AlSi_xN_y$ embedded layer for attenuated phase-shifting mask in 193 nm and the modification of the $R-T$ method for measuring n and k

Cheng-ming Lin and Wen-an Loong[a]
Institute of Applied Chemistry, National Chiao Tung University, Hsinchu 300-10, Taiwan, Republic of China

(Received 1 June 2000; accepted 23 August 2000)

The formation and variation of AlN, Si_3N_4, and nitride compositions in $AlSi_xN_y$ ($x \sim 0.31$, $y \sim 0.51$) embedded material have been shown to correlate with its optical properties. The increasing content of AlN, Si_3N_4, and nitrides will increase n and decrease k of $AlSi_xN_y$. A simple and effective correction of measured reflectance $R\%$ and transmittance $T\%$ based on scalar scattering theory has been applied to the $R-T$ method for determining n and k of embedded layers for 193 nm lithography masks. A 0.2 μm etched pattern of an $AlSi_xN_y$ embedded layer on an oxide/Si wafer substrate was successfully fabricated. © *2000 American Vacuum Society.*
[S0734-211X(00)08906-X]

I. INTRODUCTION

Compared to spin-on-glass or etched quartz attenuated phase-shifting mask (AttPSM), a single embedded layer AttPSM is more attractive because of the merits of easier fabrication, inspection, and repair.[1] Many embedded materials for AttPSM blank for ArF 193 nm lithography have been reported, among them, MoSiO,[2] SiN,[3,4] ZrSiO,[5,6] TaSiO,[7] CrAlO,[8] and CrF,[8,9] are more important and most studied.

MoSiO has good etching selectivity, but lack of exposure durability. SiN has good moisture and exposure durability, but showed a low conductivity and rough surface after etching. ZrSiO is a promising material especially in Japan, however, the $R\%$ (reflectance) at 193 nm is larger than 25%, a little higher than expected. TaSiO has a reasonable etching selectivity over quartz substrate, but not over resist. CrAlO shows chemical and exposure stabilities, but the etching selectivity is not quite known. CrF will degrade in humidity and ArF laser irradiation.

However, the effect of the chemical compositions on the optical properties of these embedded materials has not been well studied. The influence of the chemical composition is certainly critical to the optical and physical properties of embedded layers. We have reported several materials which have potential as embedded layer of AttPSM for 193 nm lithography in recent years.[10–12] In this article, the correlation between the chemical composition and the optical properties of $AlSi_xN_y$ embedded layers formed by different deposition conditions is presented. Three analysis techniques, electron spectroscopy for chemical analysis (ESCA), electron probe x-ray microanalyzer (EPMA), and Fourier transform-infrared (FT-IR), were used to study the correlation. Helicon wave etcher and Taguchi methodology of design of experiment were also employed to study the etching selectivity of the embedded layer over fused silica substrate and chemically amplified NEB-22 negative resist. Under the optimized etching conditions in our study, a 0.2 μm etched pattern of $AlSi_xN_y$ on an oxide/Si wafer substrate has been successfully fabricated. A simple and effective correction of measured $R\%$ (reflectance) and $T\%$ (transmittance) applied to the $R-T$ method for calculating n (refractive index) and k (absorption coefficient, extinction coefficient) of an embedded layer at 193 nm is also presented.

II. EXPERIMENT

$AlSi_xN_y$ films were formed by plasma sputtering of Al (100–130 W), Si (20–50 W) under Ar (75 sccm) and nitrogen (2.5–6 sccm) with an Ion Tech Merovac 450C sputtering system. The $R\%$ and $T\%$ were taken from a Shimadsu UV-2501PC double-beam ultraviolet (UV)-visible (VIS) spectrometer. Our modified $R-T$ method and an n&k Technology NKT 1200 analyzer were used for the determination of n and k of thin films. The thickness of the embedded layer and fused silica was measured using a Dektak 3030 surface profilometer and a Hitachi S-400 field emission (FE)-scanning electron microscope (SEM). The resist thickness was measured with a Nano Spec/AFT Models 210UV thin film measurement system. The ion depth profiles of embedded materials were analyzed by a Cameca IMS-5F secondary ion mass spectrometer (SIMS) using O_2^+ as ion source under 12.5 kV and 1/20 000 atomic unit resolution. Sheet resistance was measured using a Napson RT-7 resistance analyzer. The SEM micrographs were taken by a Hitachi S-400 FE–SEM and a S-6260H in-line CC–FE SEM. Atomic force microscope (AFM) used is a Digital Instruments D5000. The chemical compositions of thin film were analyzed with a Physical Electronics PHI 1600 ESCA using Mg K_α standard source with a scan resolution of 0.2 eV. The atomic ratio of thin films was measured with a Jeol JXA-8800M EPMA. The IR spectra of embedded materials were obtained from thin films deposited on Si substrate and measured with a Shimadsu FT-IR 8300 spectrometer.

Three different resists, chemically amplified NEB-22

[a]Electronic mail: loong@cc.nctu.edu.tw

Redistribution subject to AVS license or copyright; see http://scitation.aip.org/termsconditions. Download to IP: 140.113.38.11 On: Thu, 01 May 2014 07:40:58

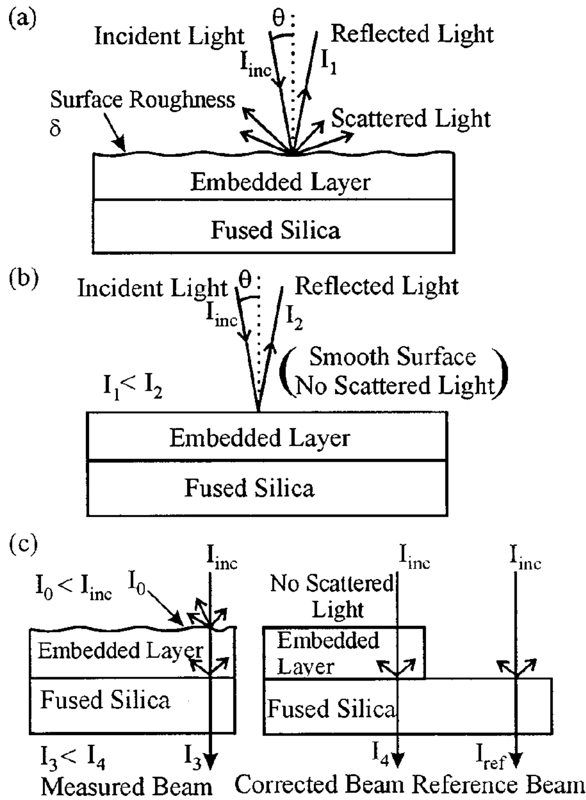

(d) R% Approximate Correction Equation

Measured R% = $(I_1 / I_{inc}) \times 100\%$

Corrected R% = $(I_2 / I_{inc}) \times 100\%$

$I_1 = I_2 \exp[-(4\pi\delta\cos\theta/\lambda)^2]$ $(I_2 > I_1)$

Corrected R% = Measured R% $/\exp[-(4\pi\delta\cos\theta/\lambda)^2]$

$(\theta = 8°)$

(Corrected R% > Measured R%)

(e) T% Approximate Correction Equation

Measured T% = $(I_3 / I_{ref}) \times 100\%$

Corrected T% = $(I_4 / I_{ref}) \times 100\%$

$(I_4 / I_3) \sim (I_{inc} / I_0)$ $(I_4 > I_3,\ I_{inc} > I_0)$

$I_0 \sim I_{inc} \exp[-(4\pi\delta\cos\theta/\lambda)^2]$

$I_4 \sim I_3 / \exp[-(4\pi\delta\cos\theta/\lambda)^2]$

Corrected T% ~ Measured T% $/ \exp[-(4\pi\delta\cos\theta/\lambda)^2]$

Corrected T% ~ Measured T% $/ \exp[-(4\pi\delta/\lambda)^2]$

$(\theta = 0°)$

(Corrected T% > Measured T%)

I_0: Light intensity on the surface of embedded layer

δ: Root-mean-square surface roughness (unit: nm)

λ: Wavelength of incident light (unit: nm)

FIG. 1. Illustration of principle of approximate corrections of measured $R\%$ and $T\%$ in the $R-T$ method for determining n and k of embedded layer and the correction equations used.

negative resist (Sumitomo), electron (e)-beam ZEP-520 positive resist and conventional DQN (DQ+Novolac) positive resist, were used to evaluate the plasma durability and the etching selectivity over $AlSi_xN_y$. The lithographic patterning of resist on $AiSi_xN_y$ was carried out by a Leica EBML-300 e-beam exposure system. An Anelva ILD-4100 helicon wave

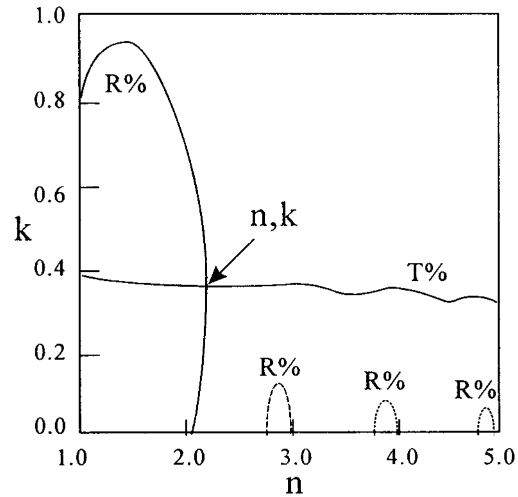

FIG. 2. n, k plot from the $R-T$ method.

etcher using O_2+BCl_3/Cl_2 was employed to study etching selectivity and patterning of the $AlSi_xN_y$ embedded layer.

III. RESULTS AND DISCUSSION

A. Modification of the $R-T$ method

Theoretically, the surface of the embedded layer is considered to be absolutely smooth in the $R-T$ method.[13] Only reflected light (with same angle as incident light) with no scattered or stray light is generated from the surface of an embedded layer. In practice, the surface of an embedded layer deposited by sputtering is rough and not smooth. The measured $R\%$, taken directly from an UV–VIS spectrometer, does not include scattered light. The real $R\%$ is a little higher than the measured $R\%$ and should be used in the calculation of the $R-T$ method. The approximate correction of the measured $R\%$ to real $R\%$ is based on scalar scattering theory.[14] The illustration and approximate correction equation of $R\%$ are shown in Figs. 1(a), 1(b), and 1(d). The important parameter δ (root-mean-square surface roughness) in the correction equation can be measured with an AFM.

Similarly, the real $T\%$ is also a little higher than the measured $T\%$ and should be used in the calculation of the $R-T$ method. The illustration and approximate correction equation

TABLE I. Comparison of n, k of a Si_xN_y film as a testing sample determined by the modified $R-T$ method and from an $n\&k$ analyzer. Wavelength=193 nm. Film thickness=73.4 nm. Root-mean-square surface roughness δ =1.7 nm. n of fused silica=1.561 (under 193 nm wavelength). d_{180}: Calculated film thickness with 180° phase-shift. (%): The deviation from value measured by an $n\&k$ analyzer.

	$T\%$	$R\%$	n	k	d_{180} (nm)
$T\%$, $R\%$ as measured	5.61	18.19	2.395(−1.6%)	0.550(+1.5%)	69.18
$R\%$ corrected only	5.61	18.41	2.425(−0.5%)	0.550(+1.5%)	67.72
$T\%$, $R\%$ corrected	5.68	18.41	2.433(−0.2%)	0.543(+0.2%)	67.34
By $n\&k$ analyzer			2.437	0.542	67.15

Redistribution subject to AVS license or copyright; see http://scitation.aip.org/termsconditions. Download to IP: 140.113.38.11 On: Thu, 01 May 2014 07:40:58

TABLE II. *n*, *k* of an $AlSi_xN_y$ film obtained from the modified *R–T* method. Wavelength=193 nm. Film thickness=98.1 nm. Root-mean-square surface roughness δ=2.7 nm. *n* of fused silica=1.561 (under 193 nm wavelength).

	$T\%$	$R\%$	n	k	d_{180} nm
$T\%$, $R\%$ as measured	6.20	12.26	2.005	0.410	96.02
$R\%$ corrected only	6.20	12.64	2.034	0.410	93.33
$T\%$, $R\%$ corrected	6.36	12.64	2.037	0.401	93.06

of $T\%$ are shown in Figs. 1(c), and 1(e). The *n, k* plot from the $R-T$ method is shown in Fig. 2. The *n, k* are determined from the intersection of R, T curves.

The comparison of the *n* and *k* of a Si_xN_y thin film at 193 nm wavelength as a testing sample determined from our modified $R-T$ method and from a commercial available $n\&k$ analyzer was shown in Table I. Since Si_xN_y thin film is one of the built-in materials of $n\&k$ analyzer, the n,k data obtained should be quite reliable. After the correction of both $R\%$ and $T\%$, the *n* and *k* of Si_xN_y thin film are quite close to the value obtained from the $n\&k$ analyzer. The results demonstrated that our corrections of $R\%$ and $T\%$ applied to the $R-T$ method for measuring *n* and *k* of a thin film are simple and effective. UV–VIS spectrometer is less expensive and available in most labs, the expensive variable angle spectroscopic ellipsometer may not be used for measuring *n* and *k* of a thin film at 193 nm or other wavelengths.

Since $AlSi_xN_y$ thin film is not the built-in material of this $n\&k$ analyzer, the significant and reliable values of *n* and *k* could not be obtained. However, *n* and *k* of $AlSi_xN_y$ thin film can be obtained by our modified $R-T$ methods, the results were summarized in Table II. We have confidence that these values are reliable.

B. Correlation between chemical compositions and optical properties of $AlSi_xN_y$ films

The optical and physical properties of $AlSi_xN_y$ ($x\sim0.31$, $y\sim0.51$) thin films formed by sputtering are suitable to be used as an embedded layer for 193 nm lithography. The *n, k* plane of $AlSi_xN_y$ at 193 nm is illustrated in Fig. 3.

The effect of atomic percentage of nitrogen on *n* and *k* of $AlSi_xN_y$ is shown in Fig. 4. The *n* and *k* data with error bars measured from the modified $R-T$ method were fitted to second order polynomial function. The measurements of *n* and *k* show a 0.5%–1.5% deviation from the point of average at

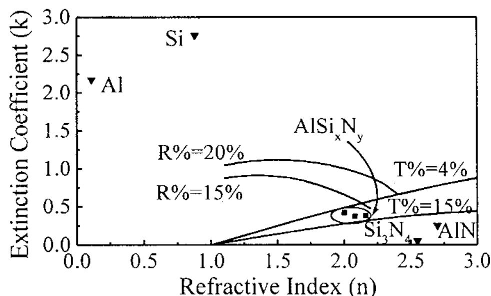

FIG. 3. *n, k* plane of $AlSi_xN_y$ embedded material in 193 nm.

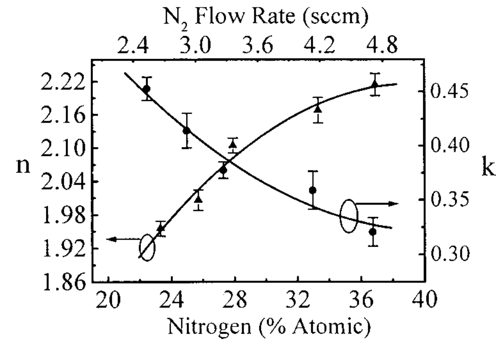

FIG. 4. Effect of nitrogen atomic % on *n* & *k* of $AlSi_xN_y$ deposited under Al 130 W, Si 40 W, Ar 75 sccm, and N_2 2.5–5.6 sccm.

specific atomic percentage. With increasing of nitrogen content, more Si and Al nitride structures form, leading to higher *n* and lower *k*. The AlN, Si_3N_4, and other nitrides having lower *k* and higher *n* as is generally known. The change of *n* and *k* is quite smooth with the nitrogen flow rate.

With the increasing of nitrogen flow rate, the variations of ESCA peak height of nitrides (N 1s, 397.9 eV), AlN (Al 2p, 75.3 eV), Al (Al 2p, 73.1 eV),[15] Si_3N_4 (Si 2p, 102.4 eV), and Si (Si 2p, 99.2 eV) are shown in Fig. 5. At about 5 sccm N_2 flow rate, the Al metallic state nearly disappeared, and the saturation of formation of AlN is observed. Similarly to formation of AlN, at about 4.5 sccm N_2 flow rate, nearly all the Si was transformed to Si_3N_4, and the saturation of formation of Si_3N_4 was also observed. At about 80 W of direct current (dc) power of Al target, only AlN and no Al metallic state appeared in ESCA as shown in Fig. 6. At about 100 W, Al metallic state started to appear. This is another proof of the saturation of formation of AlN. At about 60 W of radio frequency (rf) power of Si target, Si started to appear, saturation of formation of Si_3N_4 was clear as also shown in Fig. 6. The oxygen atom was not detected by SIMS in $AlSi_xN_y$ films.

The FT-IR spectra of $AlSi_xN_y$ films also indicated higher AlN (665 cm^{-1})[16] and Si_3N_4 (875 cm^{-1}) absorption bands with the increasing of nitrogen flow rate as shown in Fig. 7.

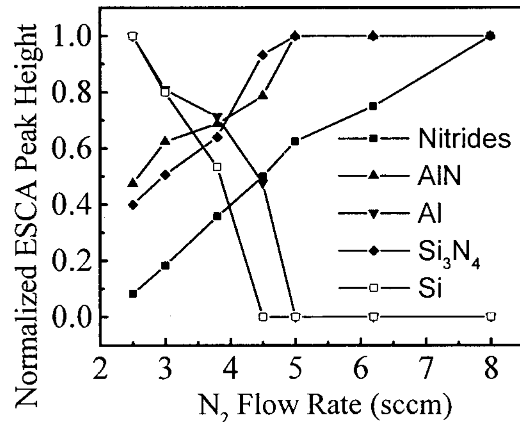

FIG. 5. Variations of the normalized ESCA peak height of nitride, AlN, Al, Si_3N_4, and Si compositions in $AlSi_xN_y$ against N_2 flow rates under Al 130 W, Si 40 W, and Ar 75 sccm.

Redistribution subject to AVS license or copyright; see http://scitation.aip.org/termsconditions. Download to IP: 140.113.38.11 On: Thu, 01 May 2014 07:40:58

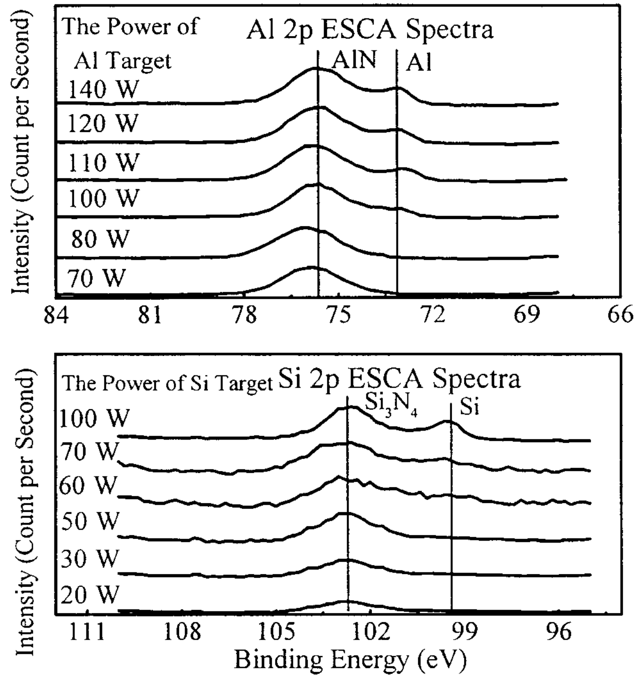

FIG. 6. ESCA spectra showing the effect of the dc power of Al target on the formation of AlN in $AlSi_xN_y$ deposited under Al 70–140 W, Si 40 W, Ar 75 sccm, and N_2 3.5 sccm.

The trends observed with ESCA were also observed by FT-IR. The broadening of these two absorption bands was due to the complicated nitrogen bonding arrangements at Al and Si atom sites. Besides the formations of AlN and Si_3N_4, the $AlSi_x$ composition may also exist in $AlSi_xN_y$,[17] however, this composition has not yet been proven in this study.

Because of the expensive ArF 193 nm laser is not available, a ~254 nm broadband deep UV light was used instead to examine the exposure durability of $AlSi_xN_y$. With irradiation doses up to 1.2×10^3 J/cm^2, optical properties of $AlSi_xN_y$ showed only a very slight change.

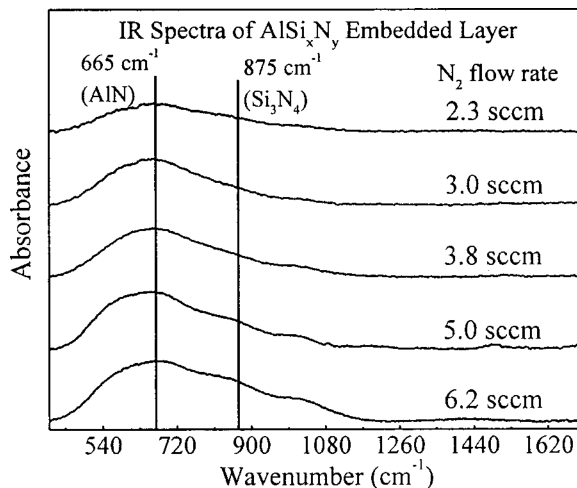

FIG. 7. FT-IR spectra showing the effect of N_2 flow rate on the formation of AlN and Si_3N_4 in $AlSi_xN_y$.

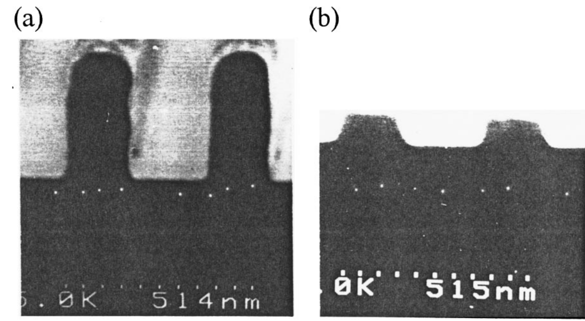

FIG. 8. SEM of (a) 0.15 μm line/space (1:1) of NEB-22 negative resist pattern on the $AlSi_xN_y$ embedded layer and (b) 0.2 μm line/space (1:1) etched pattern of $AlSi_xN_y$ on oxide/Si wafer substrate.

C. Etching properties and etched patterns

The Leica EBML-300 e-beam exposure system, helicon wave etcher using $BCl_3/Cl_2/O_2$ mixed gases, chemically amplified negative resist NEB-22, and L9 (four factors and three levers, nine experiments) orthogonal arrays of Taguchi method were employed to investigate the dry etching characteristics of $AlSi_xN_y$ as an embedded layer for AttPSM. Under chamber pressure 3 mTorr, BCl_3 45 sccm, Cl_2 7 sccm, plasma source power 1400 W, and substrate bias rf power 30 W, the selectivity of $AlSi_xN_y$ over NEB-22 resist was found to be 4.8:1. The selectivity of $AlSi_xN_y$ over fused silica was 12.3:1 under chamber pressure 9 mTorr, BCl_3 13 sccm, Cl_2 45 sccm, O_2 8 sccm, plasma source power 1400 W, and substrate bias rf power 30 W. A 0.15 μm linewidth resist pattern and 0.2 μm linewidth etched pattern of an $AlSi_xN_y$ embedded layer on an oxide/Si wafer substrate was successfully fabricated as illustrated in Fig. 8.

IV. CONCLUSIONS

With formations of AlN and Si_3N_4, resulted the higher n and lower k to $AlSi_xN_y$. The correlation between the chemical compositions and the optical properties of $AlSi_xN_y$ embedded layer was demonstrated. A 0.2 μm line/space (1:1) etched pattern of an $AlSi_xN_y$ embedded layer on an oxide/Si wafer substrate was successfully fabricated. The approximate corrections of R% and T% for measuring n and k by the $R-T$ method are also demonstrated as a simple and significant modification of the $R-T$ method.

ACKNOWLEDGMENT

This work was financially supported by the National Science Council, Republic of China, under Contract No. NSC 89-2215-E-009-026.

[1] U. Ushioda *et al.*, Jpn. J. Appl. Phys., Part 1 **35**, 6356 (1996).
[2] B. W. Smith *et al.*, Microelectron. Eng. **35**, 201 (1997).
[3] Z. T. Jiang *et al.*, Jpn. J. Appl. Phys., Part 1 **37**, 571 (1998).
[4] H. L. Chen, L. A. Wang, and C. W. Hsu, J. Vac. Sci. Technol. B **16**, 3612 (1998).
[5] T. Matsuo *et al.*, Jpn. J. Appl. Phys., Part 1 **38**, 7004 (1999).
[6] T. Matsuo *et al.*, Proc. SPIE **3096**, 354 (1997).
[7] B. W. Smith *et al.*, J. Vac. Sci. Technol. B **15**, 2259 (1997).
[8] E. Kim *et al.*, Appl. Opt. **36**, 7247 (1997).

Redistribution subject to AVS license or copyright; see http://scitation.aip.org/termsconditions. Download to IP: 140.113.38.11 On: Thu, 01 May 2014 07:40:58

[9]E. Kim *et al.*, Appl. Opt. **37**, 4254 (1998).
[10]W. A. Loong *et al.*, Microelectron. Eng. **41/42**, 125 (1998).
[11]C. M. Lin and W. A. Loong, Microelectron. Eng. **46**, 93 (1999).
[12]W. A. Loong and C. M. Lin, Microelectron. Eng. **53**, 133 (2000).
[13]R. T. Philip, J. Phys. D **16**, 489 (1983).
[14]J. M. Bennett and L. Mattsson, *Introduction to Surface Roughness and Scattering* (Optical Society of America, Washington, DC, 1993), p. 50.
[15]Y. Watanabe *et al.*, J. Vac. Sci. Technol. A **17**, 603 (1999).
[16]D. Manova *et al.*, Surf. Coat. Technol. **106**, 205 (1998).
[17]X. B. Wang and L. S. Wang, J. Chem. Phys. **107**, 7667 (1997).

Redistribution subject to AVS license or copyright; see http://scitation.aip.org/termsconditions. Download to IP: 140.113.38.11 On: Thu, 01 May 2014 07:40:58